tetrahedrally coordinated Fe. The Mössbauer shift for octahedral Fe^{2+} appears to be 0.90 mm/s. Knowledge of isomer shifts for the compounds $Fe[S_2CN(n\text{-}Bu)_2]_3$ and $Fe[S_2CN(CH_2)_4]_3$, in which iron atoms are in the trivalent oxidation state, would be extremely valuable in order to establish its variation with valence in octahedrally coordinated iron compounds.

Acknowledgment. Financial support for this research effort by the National Science Foundation and the Robert A. Welch Foundation, Houston, Tex., is gratefully acknowledged. The comments of Dr. R. D. Shannon have been very helpful in the preparation of this manuscript, and we wish to thank him also for communicating to us his results on Fe_2SiS_4 and Fe_2GeS_4 prior to their publication.

Registry No. $Ba_6Fe_8S_{15}$, 37204-48-1; Ba_2FeS_3, 37204-45-8; $BaFe_2S_3$, 37204-43-6; $Ba_7Fe_6S_{14}$, 12537-50-7; Ba_3FeS_5, 58915-68-7; $Ba_{15}Fe_7S_{25}$, 58915-69-8; $Ba_5Fe_9S_{18}$, 53810-48-3; $CuFeS_2$, 1308-56-1; Cu_2FeSnS_4, 12019-29-3; $CuFe_2S_3$, 12140-08-8; $KFeS_2$, 12022-42-3; $RbFeS_2$, 12140-50-0; $CsFeS_2$, 12158-53-1; $NaFeS_2$, 12160-05-3; $FeCr_2S_4$, 12018-12-1; $FeIn_2S_4$, 12292-75-0; Fe_2SiS_4, 59123-33-0; Fe_2GeS_4, 12332-32-0; Fe_7S_8, 12063-67-1; FeS, 1317-37-9; Fe_3S_4, 12063-38-6; $[(n\text{-}Bu)_4N]_2[FeS_2(CH_2)_2]_2$, 36841-25-5; $(n\text{-}Bu)_4NFe[S_2C_2(CN)_2]_2$, 31358-28-8; $[Ph_4As]_2Fe[S_2C_2(CN)_2]_3$, 25595-40-8; $Fe[S_2CN(n\text{-}Bu)_2]_3$, 14526-32-0; $Fe[S_2CN(CH_2)_4]_3$, 21288-86-8; $Fe\{[SP(CH_3)_2]_2N\}_2$, 29950-57-0; $[Ph_4As]_2Fe_4S_4[S_2C_2(CF_3)_2]_4$, 12572-53-1; $(Et_4N)_2[Fe_4S_4(SCH_2Ph)_4]$, 50923-41-6.

References and Notes

(1) I. E. Grey, H. Hong, and H. Steinfink, *Inorg. Chem.*, **10**, 340 (1971).
(2) H. Hong, I. E. Grey, and H. Steinfink, *Natl. Bur. Stand. (U.S.), Spec. Publ.*, No. 364 (1972).
(3) H. Hong and H. Steinfink, *J. Solid State Chem.* **5**, 93 (1972).
(4) W. M. Reiff, I. E. Grey, A. Fan, Z. Eliezer, and H. Steinfink, *J. Solid State Chem.*, **13**, 32 (1975).
(5) J. T. Lemley, J. M. Jenks, J. T. Hoggins, Z. Eliezer, and H. Steinfink, *J. Solid State Chem.*, **16**, 117 (1976).
(6) M. B. Robin and P. Day, *Adv. Inorg. Chem. Radiochem.* **10**, 247 (1967).
(7) I. D. Brown and R. D. Shannon, *Acta Crystallogr., Sect. A*, **29**, 266 (1973).
(8) R. W. G. Wyckoff, "Crystal Structures", Wiley-Interscience, New York, N. Y., 1963.
(9) A. Davidson and E. S. Switkes, *Inorg. Chem.*, **10**, 837 (1971).
(10) V. W. Bronger, *Z. Anorg. Allg. Chem.*, **359**, 225 (1968).
(11) S. R. Hall and J. M. Stewart, *Acta Crystallogr., Sect. B*, **29**, 579 (1973).
(12) N. E. Erickson, *Adv. Chem. Ser.*, **No. 68**, 86 (1967).
(13) P. C. Healy and A. H. White, *Chem. Commun.*, 1446 (1971).
(14) J. Danon, "Chemical Applications of Mössbauer Spectroscopy", V. I. Gol'danskii and R. H. Herber, Ed., Academic Press, New York, N. Y., 1963, Chapter 3.
(15) J. G. Norman, Jr., and S. C. Jackels, *J. Am. Chem. Soc.*, **97**, 3833 (1975).
(16) J. G. Norman, Jr., private communication.
(17) T. Teranishi, *J. Phys. Soc. Jpn.*, **16**, 1881 (1961).
(18) E. F. Bertaut, P. Burlet, and J. Chappert, *Solid State Commun.*, **3**, 335 (1965).
(19) D. J. Vaughan and M. S. Ridout, *J. Inorg. Nucl. Chem.*, **33**, 741 (1971).
(20) I. E. Grey, *Acta Crystallogr., Sect. B*, **31**, 45 (1975).
(21) S. Takeno, K. Masumoto, and T. Kamigaichi, *J. Sci. Hiroshima Univ., Ser. C*, **5**, 341 (1968).
(22) L. O. Brockway, *Z. Kristallogr., Kristallgeom., Kristallphys., Kristallchem.*, **89**, 434 (1934).
(23) M. E. Fleet, *Z. Kristallogr., Kristallgeom., Kristallphys., Kristallchem.*, **132**, 276 (1970).
(24) D. Raj and S. P. Puri, *J. Chem. Phys.*, **50**, 3184 (1969).
(25) D. O. Cowan, G. Pasternak, and F. Kaufman, *Proc. Natl. Acad. Sci. U.S.A.*, **66**, 843 (1970).
(26) M. R. Spender and A. H. Morrish, *Can. J. Phys.*, **50**, 1125 (1972).
(27) H. Hahn and W. Klinger, *Z. Anorg. Allg. Chem.*, **263**, 177 (1950).
(28) H. Vincent, E. F. Bertaut, W. H. Baur, and R. D. Shannon, to be submitted for publication.
(29) R. D. Shannon, private communication.
(30) M. Tokonami, K. Nishiguchi, and N. Morimoto, *Am. Mineral.*, **57**, 1066 (1972).
(31) D. J. Vaughan and M. S. Ridout, *Solid State Commun.*, **8**, 2165 (1970).
(32) M. E. Fleet, *Acta Crystallogr., Sect. B*, **27**, 1864 (1971).
(33) H. T. Evans, Jr., *Science*, **167**, 621 (1970).
(34) A. F. Andresen, *Acta Chem. Scand.*, **14**, 919 (1960).
(35) S. Hafner and M. Kalvius, *Z. Kristallogr., Kristallgeom., Kristallphys., Kristallchem.*, **123**, 443 (1966).
(36) B. J. Skinner, R. C. Erd, and F. S. Grimaldi, *Am. Mineral.*, **49**, 543 (1964).
(37) J. M. D. Coey, M. R. Spender, and A. H. Morrish, *Solid State Commun.*, **8**, 1605 (1970).
(38) M. R. Snow and J. A. Ibers, *Inorg. Chem.*, **12**, 249 (1973).
(39) W. C. Hamilton and I. Bernal, *Inorg. Chem.*, **6**, 2003 (1967).
(40) N. N. Greenwood and H. J. Whitfield, *J. Chem. Soc. A*, 1697 (1968).
(41) A. Sequeira and I. Bernal, *J. Cryst. Mol. Struct.*, **3**, 157 (1973).
(42) B. F. Hoskins and B. P. Kelly, *Chem. Commun.*, 1517 (1968).
(43) P. C. Healy and A. H. White, *J. Chem. Soc. A*, 1163 (1972).
(44) M. R. Churchill and J. Wormald, *Inorg. Chem.*, **10**, 1778 (1971).
(45) I. Bernal, B. R. Davis, M. L. Good, and S. Chandra, *J. Coord. Chem.*, **2**, 61 (1972).
(46) T. Herskovitz, B. A. Averill, R. H. Holm, J. A. Ibers, W. D. Phillips, and J. F. Weiker, *Proc. Natl. Acad. Sci. U.S.A.*, **69**, 2437 (1972).

Contribution from the Department of Chemistry, University of Notre Dame, Notre Dame, Indiana 46556

Molecular Stereochemistry of Two Intermediate-Spin Complexes. Iron(II) Phthalocyanine and Manganese(II) Phthalocyanine

JOHN F. KIRNER, W. DOW, and W. ROBERT SCHEIDT*

Received January 15, 1976 AIC600426

The molecular stereochemistry of iron(II) phthalocyanine and manganese(II) phthalocyanine has been determined by x-ray diffraction methods. The phthalocyanine ligand constrains the metal ion to effectively square-planar coordination and to an intermediate spin state. The Fe^{II}–N bond distance of 1.926 (1) Å and the Mn^{II}–N bond length of 1.938 (3) Å are wholly consistent with the assignment of an intermediate-spin ground state. Both complexes crystallize as the β polymorph. Crystal data are as follows: for FePc, space group $P2_1/a$, a = 19.392 (5) Å, b = 4.786 (2) Å, c = 14.604 (4) Å, β = 120.85 (1)°, ρ_{exptl} = 1.61 g/cm^3, ρ_{calcd} = 1.623 g/cm^3 for Z = 2, required molecular symmetry $\bar{1}$; for MnPc, space group $P2_1/a$, a = 19.400 (4) Å, b = 4.761 (2) Å, c = 14.613 (3) Å, β = 120.74 (1)°, ρ_{exptl} = 1.61 g/cm^3, ρ_{calcd} = 1.625 g/cm^3 for Z = 2, required molecular symmetry $\bar{1}$. Intensity data were measured by θ–2θ scanning on a Syntex $P\bar{1}$ automated diffractometer using graphite-monochromated Mo Kα radiation. For FePc, the intensities of 3949 reflections with (sin θ)/$\lambda \leq$ 0.817 Å^{-1} were used in the refinement of the 187 structural parameters and for MnPc the intensities of 2158 reflections having (sin θ)/λ < 0.69 Å^{-1} were employed. Final discrepancy indices are as follows: FePc, R_1 = 0.045, R_2 = 0.057; MnPc, R_1 = 0.066, R_2 = 0.066.

Iron(II) and manganese(II) phthalocyanine have been recognized as examples of a rare type of coordination compound in which the metal ion has an intermediate-spin ground state (Fe, S = 1; Mn, S = $^3/_2$).[1] The basic stereochemistry of four-coordinate phthalocyanines has been known for some time,[2,3] but surprisingly the quantitative stereochemistry of the much studied iron(II) and manganese(II) derivatives has not been determined. We report herein the structures of

Table I. Summary of Crystal Data and Intensity Collection

Compd	$MnN_8C_{32}H_{16}$	$FeN_8C_{32}H_{16}$
a, Å	19.400 (4)	19.392 (5)
b, Å	4.761 (2)	4.786 (2)
c, Å	14.613 (3)	14.604 (4)
β, deg	120.74 (1)	120.85 (1)
V, Å^3	1160.0	1163.7
Z	2	2
Density, g/cm^3	1.625 (calcd) 1.61 (obsd)	1.623 (calcd) 1.61 (obsd)
Space group	$P2_1/a$	$P2_1/a$
Crystal dimensions, mm	0.77 × 0.13 × 0.10	0.90 × 0.33 × 0.30
Temp, °C	20 ± 1	20 ± 1
Radiation	Graphite-monochromated Mo Kα (λ 0.710 69 Å)	Graphite-monochromated Mo Kα (λ 0.710 69 Å)
μ, mm^{-1}	0.586	0.688
Scan range	0.8° below $K\alpha_1$ to 1.0° above $K\alpha_2$	1.0° below $K\alpha_1$ to 1.0° above $K\alpha_2$
Backgrounds	Profile analysis	Profile analysis
2θ limits, deg	3.5–58.7	3.5–71°
Unique data used, $F_o > 3\sigma(F_o)$	2158	3949
Final no. of variables	187	187

MnPc[4] and FePc and compare them with the recently reported structures of the related four-coordinate iron(II)[5] and manganese(II)[6] metalloporphyrins. Differences in structure between intermediate-spin MnPc, FePc, and FeTPP and high-spin MnTPP are wholly consistent with the assigned ground states of the complexes.

Experimental Section

FePc[7] and MnPc[8] were prepared by published procedures and purified by vacuum sublimation. Single crystals, suitable for diffraction analysis, were grown by vacuum sublimation in quartz tubes at ~450 °C under a nitrogen atmosphere (reduced pressure). Crystals used in the structure analysis were cut from larger needles. Some difficulty was experienced in obtaining satisfactory crystals of MnPc.

Preliminary photographic examination by Weissenberg photography, Cu Kα radiation, showed that MnPc and FePc crystallized as the monoclinic β polymorph. The space group $P2_1/a$ [C_{2h}^5, No. 14],[9] a nonstandard choice, was chosen to conform with earlier choices of the unit cells of four-coordinate phthalocyanines.[3] Lattice constants (Table I) came from a least-squares refinement that utilized the setting angles of 30 reflections (FePc) or 60 reflections (MnPc) given by the automatic centering routine supplied with the Syntex $P\bar{1}$ diffractometer.

X-ray intensity data were collected using graphite-monochromated Mo Kα radiation on a computer-controlled four-circle diffractometer, using θ–2θ scanning, to the 2θ limits listed in Table I. Background counts were estimated from an analysis of the reflection profiles using a local modification of a program recently described.[10] Four standard reflections, measured every 50 reflections during data collection, showed no trend with exposure to the x-ray beam. Although the linear absorption coefficients (Table I) are not large, an empirical absorption correction was applied to the data.[11] Intensity data were reduced and standard deviations were calculated as described previously.[12] Data were retained as objectively observed if $F_o > 3\sigma(F_o)$, leading to 2158 unique observed data for MnPc (68% of the theoretical number possible) and 3949 unique data for FePc (74% of theoretical).

Atomic coordinates reported for CuPc[13] were used for the initial coordinates in the asymmetric unit of structure (half of the MPc molecule). Full-matrix least-squares refinement[14] converged smoothly using isotropic temperature factors for all atoms and standard values[15,16] for atomic form factors. Difference Fourier syntheses[17] gave electron density concentrations appropriately located for all hydrogen atom positions; these positions were idealized (C–H = 0.95 Å) with temperature factors fixed one unit higher than those of the associated carbon atoms. Subsequent refinements used anisotropic temperature factors for all heavy atoms and fixed hydrogen contributors and were carried to convergence. For both complexes, the final parameter shifts were less than 10% of the estimated standard deviation during the last cycle. For FePc, the final value of $R_1 = \sum[|F_o| - |F_c|]/\sum|F_o|$ was 0.045; that of $R_2 = [\sum w(|F_o| - |F_c|)^2/\sum w(F_o^2)]^{1/2}$ was 0.057. The estimated standard deviation of an observation of unit weight was 1.37, with a final data:parameter ratio of 21.1. A final difference Fourier had no significant features; the largest peaks were <0.75 e, or less than 10% of the height of a benzo carbon atom. For MnPc, the final value of R_1 was 0.066; that of R_2 was 0.066. The estimated standard deviation of an observation of unit weight was 1.78, with a final data:parameter ratio of 11.5. A final difference Fourier had three peaks of ~0.9 e near the manganese atom; there were otherwise no significant features.

Table II. Atom Coordinates in the FePc Unit Cell[a]

Atom	10^4x	10^4y	10^4z
Fe	0	0	0
N_1	−788 (1)	−5159 (3)	724 (1)
N_2	327 (1)	−1953 (3)	1315 (1)
N_3	1601 (1)	279 (3)	2519 (1)
N_4	969 (1)	2187 (3)	729 (1)
C_1	−97 (1)	−4053 (4)	1449 (1)
C_2	321 (1)	−4953 (4)	2552 (1)
C_3	130 (1)	−6957 (4)	3081 (1)
C_4	664 (1)	−7269 (5)	4166 (2)
C_5	1363 (1)	−5677 (5)	4706 (2)
C_6	1556 (1)	−3687 (4)	4173 (1)
C_7	1017 (1)	−3357 (4)	3084 (1)
C_8	1014 (1)	−1506 (3)	2292 (1)
C_9	1574 (1)	1964 (3)	1785 (1)
C_{10}	2209 (1)	3935 (4)	2002 (1)
C_{11}	2950 (1)	4506 (4)	2917 (1)
C_{12}	3426 (1)	6532 (5)	2833 (2)
C_{13}	3179 (1)	7960 (4)	1882 (2)
C_{14}	2443 (1)	7407 (4)	972 (1)
C_{15}	1965 (1)	5365 (3)	1053 (1)
C_{16}	1189 (1)	4248 (3)	273 (1)

[a] The figure in parentheses following each datum is the estimated standard deviation in the last significant figure.

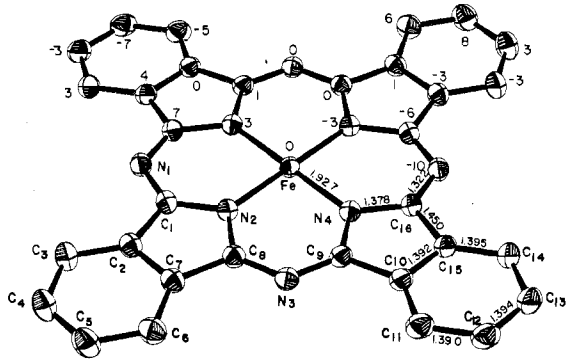

Figure 1. Computer-drawn model in perspective of the centrosymmetric FePc molecule as it exists in the crystal. On the lower half of the diagram the special symbol identifying each atom is shown. On the upper half of the figure, the symbol for each atom is replaced by its perpendicular displacement, in units of 0.01 Å, from the mean plane of the entire molecule.

A listing of the observed and calculated structure factors (×10) for MnPc and FePc is available.[18]

Atomic coordinates and the associated anisotropic thermal parameters in the asymmetric unit of structure for FePc are listed in Tables II and III; those for MnPc are listed in Tables IV and V. Primed and unprimed symbols, C_i' and C_i, represent atoms related by the center of symmetry at the origin (and the metal atom).

Results and Discussion

The numbering system employed in Tables II–XI for the carbon and nitrogen atoms in the asymmetric unit of structure is displayed in Figures 1 and 2. These figures are computer-drawn models[19] in perspective of the centrosymmetric FePc and MnPc molecules. On the upper half of each centrosymmetric figure, the special symbol identifying each atom has been replaced by the value of the perpendicular displacement of the atom, in units of 0.01 Å, from the mean plane

Table III. Thermal Parameters for FePc

Atom type	Anisotropic parameters,[a] Å²						B,[b] Å²
	B_{11}	B_{22}	B_{33}	B_{12}	B_{13}	B_{23}	
Fe	1.86 (1)	1.86 (1)	1.79 (1)	−0.12 (1)	0.92 (1)	0.10 (1)	1.84
N_1	2.28 (4)	2.36 (5)	2.21 (4)	−0.23 (4)	1.22 (4)	0.14 (4)	2.23
N_2	2.06 (4)	1.95 (4)	2.00 (4)	−0.03 (3)	1.07 (3)	0.13 (3)	1.98
N_3	2.21 (4)	2.28 (5)	1.94 (4)	−0.11 (4)	0.96 (3)	0.01 (4)	2.18
N_4	2.02 (4)	1.96 (4)	1.96 (4)	−0.14 (3)	1.04 (3)	0.01 (3)	1.97
C_1	2.23 (5)	2.11 (5)	2.12 (5)	0.09 (4)	1.25 (4)	0.25 (4)	2.08
C_2	2.37 (5)	2.23 (5)	2.18 (5)	0.21 (5)	1.26 (4)	0.34 (5)	2.20
C_3	2.86 (6)	2.80 (7)	2.78 (6)	−0.04 (5)	1.56 (5)	0.68 (5)	2.67
C_4	3.83 (8)	3.37 (8)	2.86 (7)	0.24 (7)	1.86 (6)	1.08 (6)	3.08
C_5	3.51 (8)	3.76 (8)	2.31 (6)	0.34 (6)	1.28 (6)	0.85 (6)	3.11
C_6	2.83 (6)	3.08 (7)	2.15 (5)	0.09 (6)	0.97 (5)	0.37 (5)	2.76
C_7	2.42 (5)	2.29 (5)	2.09 (5)	0.20 (4)	1.20 (4)	0.28 (4)	2.23
C_8	2.17 (5)	2.08 (5)	1.97 (5)	0.10 (4)	1.06 (4)	0.13 (4)	2.06
C_9	1.98 (5)	2.10 (5)	2.04 (5)	−0.17 (4)	1.04 (4)	−0.16 (4)	2.03
C_{10}	2.13 (5)	2.27 (5)	2.21 (5)	−0.27 (4)	1.14 (4)	−0.32 (4)	2.17
C_{11}	2.42 (6)	3.24 (8)	2.37 (5)	−0.42 (5)	0.97 (5)	−0.46 (5)	2.73
C_{12}	2.40 (6)	3.75 (8)	2.88 (6)	−0.82 (3)	1.20 (15)	−0.97 (6)	2.91
C_{13}	2.79 (6)	3.35 (8)	3.41 (7)	−1.15 (6)	1.97 (6)	−0.92 (6)	2.80
C_{14}	2.74 (6)	2.83 (6)	2.91 (6)	−0.73 (5)	1.76 (5)	−0.37 (5)	2.59
C_{15}	2.24 (5)	2.22 (6)	2.35 (5)	−0.35 (4)	1.35 (4)	−0.32 (4)	2.15
C_{16}	2.10 (5)	2.16 (5)	2.16 (5)	−0.19 (4)	1.24 (4)	−0.05 (4)	2.06

[a] The number in parentheses following each datum is the estimated standard deviation in the last significant figure. B_{ij} is related to dimensionless β_{ij} employed during refinement as $B_{ij} = 4\beta_{ij}/a^*_i a^*_j$. [b] Isotropic thermal parameters as calculated from $B = 4[V^2 \det(\beta_{ij})]^{1/3}$.

Table IV. Atomic Coordinates in the MnPc Unit Cell[a]

Atom type	Coordinates		
	10^4x	10^4y	10^4z
Mn	0	0	0
N_1	−772 (2)	−5268 (6)	731 (2)
N_2	331 (2)	−1985 (6)	1320 (2)
N_3	1604 (2)	304 (6)	2523 (2)
N_4	968 (2)	2239 (6)	728 (2)
C_1	−92 (2)	−4104 (8)	1448 (3)
C_2	332 (2)	−4989 (8)	2562 (3)
C_3	141 (2)	−6987 (8)	3096 (3)
C_4	669 (2)	−7273 (9)	4178 (3)
C_5	1360 (2)	−5654 (9)	4705 (3)
C_6	1553 (2)	−3679 (9)	4181 (3)
C_7	1018 (2)	−3366 (8)	3083 (3)
C_8	1025 (2)	−1500 (8)	2307 (3)
C_9	1581 (2)	1998 (7)	1791 (3)
C_{10}	2208 (2)	3995 (8)	2000 (3)
C_{11}	2952 (2)	4573 (9)	2900 (3)
C_{12}	3423 (2)	6589 (9)	2814 (3)
C_{13}	3177 (2)	8032 (9)	1867 (3)
C_{14}	2442 (2)	7482 (8)	971 (3)
C_{15}	1962 (2)	5448 (7)	1049 (3)
C_{16}	1186 (2)	4342 (7)	273 (3)

[a] The figure in parentheses following each datum is the estimated standard deviation in the last significant figure.

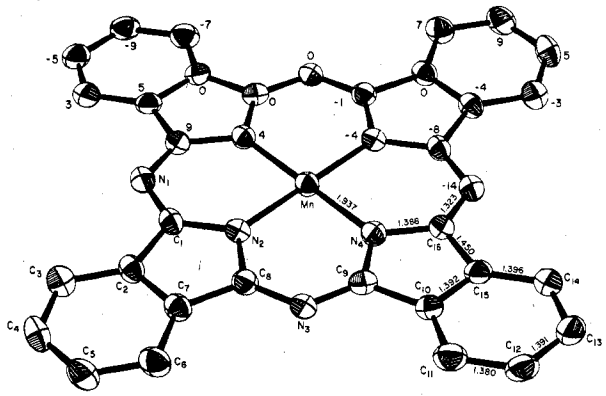

Figure 2. Computer-drawn model in perspective of the centrosymmetric MnPc molecule as it exists in the crystal. On the lower half of the diagram the special symbol identifying each atom is displayed. On the upper half of the figure, the symbol for each atom is replaced by its perpendicular displacement, in units of 0.01 Å, from the mean plane of the entire molecule.

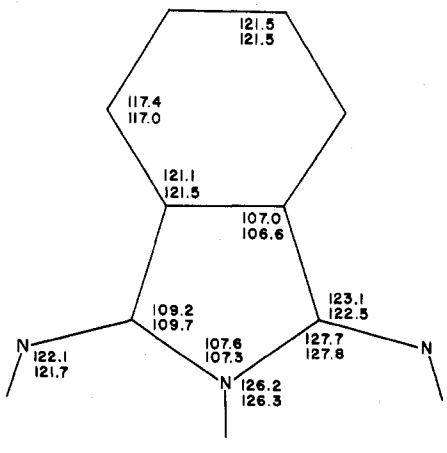

Figure 3. Formal diagram of one-fourth of a phthalocyanine molecule showing the average bond angles of each chemical type. The upper entry of each pair is the value for MnPc; the lower value is that for FePc.

of the entire molecule. Although the deviation of any atom from exact planarity is small, a comparison of Figure 1 and Figure 2 reveals that the patterns of displacements from the mean plane in FePc and MnPc are quite similar. Individual units of the macrocycle, i.e., a pyrrole ring or a benzo ring are planar to within 0.01 Å. The dihedral angles between an individual pyrrole ring and its associated benzo ring, i.e., an isoindole unit, are all less than 2°.

Individual bond parameters, with estimated standard deviations, are found in Tables VII–IX. Averaged values of bond lengths in FePc and MnPc are entered on Figures 1 and 2, respectively. Averaged values for bond angles of a given chemical type are displayed in Figure 3. Although the average bond parameters can be expected to vary slightly with the size of the central hole of the phthalocyanine ligand, values found in this study agree well with previous studies.[20,21]

The anisotropic temperature factors (Tables III and V) and the concomitant root-mean-square amplitudes of vibration (Tables X and XI[18]) are only consistent with an ordered structure that has the metal atom centered in the molecule.

Table V. Thermal Parameters for MnPc

Atom type	Anisotropic Parameters,[a] Å²						B,[b] Å²
	B_{11}	B_{22}	B_{33}	B_{12}	B_{13}	B_{23}	
Mn	2.30 (3)	2.42 (3)	1.78 (3)	−0.20 (3)	0.87 (2)	0.22 (3)	2.20
N_1	2.7 (1)	2.6 (1)	2.4 (1)	−0.2 (1)	1.4 (1)	0.1 (1)	2.5
N_2	2.4 (1)	2.3 (1)	1.9 (1)	0.0 (1)	1.1 (1)	0.0 (1)	2.2
N_3	2.6 (1)	2.4 (1)	1.9 (1)	−0.1 (1)	1.1 (1)	0.0 (1)	2.3
N_4	2.3 (1)	2.2 (1)	1.9 (1)	0.0 (1)	1.0 (1)	0.2 (1)	2.2
C_1	2.6 (1)	2.3 (1)	2.2 (1)	0.3 (1)	1.4 (1)	0.4 (1)	2.2
C_2	2.6 (1)	2.3 (1)	2.3 (1)	0.5 (1)	1.4 (1)	0.5 (1)	2.3
C_3	3.2 (2)	3.2 (2)	2.9 (2)	0.0 (1)	1.7 (1)	0.3 (1)	3.0
C_4	4.4 (2)	3.5 (2)	3.1 (2)	0.1 (2)	2.2 (2)	1.2 (2)	3.2
C_5	4.1 (2)	3.8 (2)	2.2 (1)	0.2 (2)	1.4 (1)	0.7 (1)	3.2
C_6	3.0 (2)	3.5 (2)	2.1 (1)	0.1 (1)	1.0 (1)	0.4 (1)	2.9
C_7	2.8 (1)	2.4 (2)	2.3 (1)	0.4 (1)	1.4 (1)	0.4 (1)	2.4
C_8	2.4 (1)	2.4 (2)	2.1 (1)	0.0 (1)	1.1 (1)	0.0 (1)	2.3
C_9	2.4 (1)	2.4 (2)	2.3 (1)	0.0 (1)	1.2 (1)	−0.3 (1)	2.3
C_{10}	2.6 (1)	2.3 (1)	2.4 (1)	−0.2 (1)	1.3 (1)	−0.4 (1)	2.4
C_{11}	3.1 (2)	3.6 (2)	2.3 (1)	−0.2 (1)	1.1 (1)	−0.4 (1)	3.1
C_{12}	2.7 (2)	3.8 (2)	2.8 (2)	−0.8 (1)	1.2 (1)	−1.1 (1)	3.0
C_{13}	3.3 (2)	3.4 (2)	3.7 (2)	−1.1 (1)	2.3 (1)	−1.1 (2)	3.1
C_{14}	3.2 (2)	3.0 (2)	2.8 (1)	−0.4 (1)	1.8 (1)	−0.4 (1)	2.8
C_{15}	2.5 (1)	2.4 (2)	2.4 (1)	−0.1 (1)	1.4 (1)	−0.5 (1)	2.3
C_{16}	2.5 (1)	2.3 (2)	2.3 (1)	−0.1 (1)	1.5 (1)	−0.1 (1)	2.3

[a] The number in parentheses following each datum is the estimated standard deviation in the last significant figure. B_{ij} is related to the dimensionless β_{ij} employed during refinement as $B_{ij} = 4\beta_{ij}/a^*_i a^*_j$. [b] Isotropic thermal parameters as calculated from $B = 4[V^2 \det(\beta_{ij})]^{1/3}$.

Table VI. Bond Lengths in the FePc Skeleton[a]

Type[b]	Length, Å	Type	Length, Å	Type	Length, Å
Fe-N_2	1.927 (1)	N_4-C_{16}	1.375 (2)	C_9-C_{10}	1.452 (2)
Fe-N_4	1.926 (1)	C_1-C_2	1.449 (2)	C_{10}-C_{11}	1.397 (2)
N_1-C_1	1.320 (2)	C_2-C_3	1.395 (2)	C_{10}-C_{15}	1.393 (2)
N_1-C_{16}'	1.324 (2)	C_2-C_7	1.390 (2)	C_{11}-C_{12}	1.386 (3)
N_2-C_1	1.374 (2)	C_3-C_4	1.387 (3)	C_{12}-C_{13}	1.395 (3)
N_2-C_8	1.382 (2)	C_4-C_5	1.394 (3)	C_{13}-C_{14}	1.389 (3)
N_3-C_8	1.322 (2)	C_5-C_6	1.396 (3)	C_{14}-C_{15}	1.393 (2)
N_3-C_9	1.322 (2)	C_6-C_7	1.394 (2)	C_{15}-C_{16}	1.446 (2)
N_4-C_9	1.382 (2)	C_7-C_8	1.454 (2)		

[a] The number in parentheses following each datum is the estimated standard deviation in the last significant figure. [b] C_i and C_i' denote atoms related by the center of inversion.

Table VII. Bond Angles in the FePc Skeleton[a]

Type[b]	Value, deg	Type	Value, deg	Type	Value, deg
N_2FeN_4	89.1 (1)	$C_1C_2C_7$	106.7 (1)	$N_4C_9C_{10}$	109.5 (1)
N_2FeN_4'	90.9 (1)	$C_3C_2C_7$	121.7 (2)	$C_9C_{10}C_{11}$	132.6 (2)
$C_1N_1C_{16}'$	122.1 (1)	$C_2C_3C_4$	116.9 (2)	$C_9C_{10}C_{15}$	106.5 (1)
FeN_2C_1	125.5 (1)	$C_3C_4C_5$	121.8 (2)	$C_{11}C_{10}C_{15}$	120.9 (2)
FeN_2C_8	127.2 (1)	$C_4C_5C_6$	121.2 (2)	$C_{10}C_{11}C_{12}$	117.2 (2)
$C_1N_2C_8$	107.2 (1)	$C_5C_6C_7$	117.0 (2)	$C_{11}C_{12}C_{13}$	121.8 (2)
$C_8N_3C_9$	121.3 (1)	$C_2C_7C_6$	121.3 (2)	$C_{12}C_{13}C_{14}$	121.3 (2)
FeN_4C_9	127.1 (1)	$C_2C_7C_8$	106.4 (1)	$C_{13}C_{14}C_{15}$	117.0 (2)
FeN_4C_{16}	125.4 (1)	$C_6C_7C_8$	132.2 (2)	$C_{10}C_{15}C_{14}$	121.9 (2)
$C_9N_4C_{16}$	107.4 (1)	$N_2C_8N_3$	127.5 (1)	$C_{10}C_{15}C_{16}$	106.7 (1)
$N_1C_1N_2$	127.9 (1)	$N_2C_8C_7$	109.6 (1)	$C_{14}C_{15}C_{16}$	131.4 (2)
$N_1C_1C_2$	122.1 (1)	$N_3C_8C_7$	122.9 (1)	$N_4C_{16}N_1'$	128.0 (2)
$N_2C_1C_2$	110.0 (1)	$N_3C_9N_4$	127.7 (1)	$N_4C_{16}C_{15}$	109.9 (1)
$C_1C_2C_3$	131.6 (2)	$N_3C_9C_{10}$	122.9 (1)	$N_1'C_{16}C_{15}$	122.1 (1)

[a] The number in parentheses following each datum is the estimated standard deviation in the last significant figure. [b] C_i and C_i' denote atoms related by the center of inversion.

Table VIII. Bond Lengths in the MnPc Skeleton[a]

Type[b]	Length, Å	Type	Length, Å	Type	Length, Å
Mn-N_2	1.938 (3)	N_4-C_{16}	1.383 (4)	C_9-C_{10}	1.448 (5)
Mn-N_4	1.937 (3)	C_1-C_2	1.461 (4)	C_{10}-C_{11}	1.396 (5)
N_1-C_1	1.317 (4)	C_2-C_3	1.396 (5)	C_{10}-C_{15}	1.400 (5)
N_1-C_{16}'	1.337 (4)	C_2-C_7	1.383 (5)	C_{11}-C_{12}	1.374 (5)
N_2-C_1	1.372 (4)	C_3-C_4	1.383 (5)	C_{12}-C_{13}	1.393 (5)
N_2-C_8	1.401 (4)	C_4-C_5	1.389 (6)	C_{13}-C_{14}	1.381 (5)
N_3-C_8	1.317 (4)	C_5-C_6	1.380 (5)	C_{14}-C_{15}	1.388 (5)
N_3-C_9	1.322 (4)	C_6-C_7	1.404 (4)	C_{15}-C_{16}	1.443 (5)
N_4-C_9	1.397 (4)	C_7-C_8	1.446 (5)		

[a] The number in parentheses following each datum is the estimated standard deviation in the last significant figure. [b] C_i and C_i' denote atoms related by the center of inversion.

Table IX. Bond Angles in the MnPc Skeleton[a]

Type[b]	Value, deg	Type	Value, deg	Type	Value, deg
N_2MnN_4	89.2 (1)	$C_1C_2C_7$	106.7 (3)	$N_4C_9C_{10}$	109.1 (3)
N_2MnN_4'	90.8 (1)	$C_3C_2C_7$	121.9 (3)	$C_9C_{10}C_{11}$	132.9 (3)
$C_1N_1C_{16}'$	122.0 (3)	$C_2C_3C_4$	117.0 (3)	$C_9C_{10}C_{15}$	106.9 (3)
MnN_2C_1	125.2 (2)	$C_3C_4C_5$	121.3 (3)	$C_{11}C_{10}C_{15}$	120.1 (3)
MnN_2C_8	126.9 (2)	$C_4C_5C_6$	122.0 (3)	$C_{10}C_{11}C_{12}$	117.9 (3)
$C_1N_2C_8$	107.9 (3)	$C_5C_6C_7$	117.1 (3)	$C_{11}C_{12}C_{13}$	122.0 (3)
$C_8N_3C_9$	122.2 (3)	$C_2C_7C_6$	120.7 (3)	$C_{12}C_{13}C_{14}$	120.8 (3)
MnN_4C_9	127.0 (2)	$C_2C_7C_8$	107.6 (3)	$C_{13}C_{14}C_{15}$	117.8 (3)
MnN_4C_{16}	125.7 (2)	$C_6C_7C_8$	131.6 (3)	$C_{10}C_{15}C_{14}$	121.6 (3)
$C_9N_4C_{16}$	107.3 (3)	$N_2C_8N_3$	127.3 (3)	$C_{10}C_{15}C_{16}$	106.8 (3)
$N_1C_1N_2$	128.9 (3)	$N_2C_8C_7$	108.5 (3)	$C_{14}C_{15}C_{16}$	131.6 (3)
$N_1C_1C_2$	121.9 (3)	$N_3C_8C_7$	124.2 (3)	$N_4C_{16}N_1'$	127.3 (3)
$N_2C_1C_2$	109.2 (3)	$N_3C_9N_4$	127.3 (3)	$N_4C_{16}C_{15}$	109.8 (3)
$C_1C_2C_3$	131.3 (3)	$N_3C_9C_{10}$	123.6 (3)	$N_1'C_{16}C_{15}$	122.8 (3)

[a] The number in parentheses following each datum is the estimated standard deviation in the last significant figure. [b] C_i and C_i' denote atoms related by the center of inversion.

Thus the structural data suggest a single spin state for the metal atom in the FePc and MnPc molecules rather than a mixture of spin states.

The structural parameter of principal interest for these intermediate-spin complexes is, of course, the M–N bond distance. The values found for the two unique distances in MnPc are 1.938 (3) and 1.937 (3) Å; those for FePc are 1.927 (1) and 1.926 (1) Å. The slight decrease in the M–N bond distance for FePc is consonant with the increased nuclear charge for the iron(II) atom. It is interesting to note that the Si–N distance (1.920 Å) for the very small Si(IV) atom in $PcSi[OSi(CH_3)_3]_2$[20] is not much smaller than the M–N distances in FePc and MnPc.

The Fe–N bond lengths in FePc are intermediate to those observed in two other intermediate-spin iron(II) complexes: 1.972 (4) Å in FeTPP and 1.826 (4) and 1.846 (4) Å in an octaaza[14]annuleneiron(II) complex.[22] A possible rela-

Table XII. Complexing Bond Lengths in a Sequence of Four-Coordinate Metallophthalocyanines and Metallotetraphenylporphyrins

Metal ion	d^5 Mn	d^6 Fe	d^7 Co	d^8 Ni	d^9 Cu
Phthalocyanato M-N dist, Å	1.938 (3)	1.926 (1)		~1.83	1.934 (6)
Spin state, S	$^3/_2$	1	$^1/_2$	0	$^1/_2$
Ref	*a*	*a*		*b*	*c*
Tetraphenylporphinato M-N distance, Å	>2.082	1.972 (4)	1.949 (3)	1.928 (3)	1.981 (7)
Spin state, S	$^5/_2$	1	$^1/_2$	0	$^1/_2$
Ref	*d*	*e*	*f*	*g*	*h*

[a] This work. [b] Reference 3a. [c] Reference 13. [d] Reference 6. [e] Reference 5. [f] Reference 26. [g] Reference 27. [h] Reference 28.

tionship between the observed magnetic moments and the Fe–N bond lengths has been suggested.[22] Equatorial Fe–N bond distances of ~1.92 Å were also observed in low-spin six-coordinate bis(4-methylpyridine)phthalocyanatoiron(II)[23] and indicate minimal structural changes in the equatorial plane upon addition of two axial ligands. The addition of two axial ligands to MnPc should yield a complex of similar stereochemistry. Such low-spin $MnPcL_2$ derivatives have been prepared in solution but not isolated.[24] There appear to be no intermediate-spin manganese(II) complexes of known structure for comparison. The equatorial Mn^{III}–N bond distance in the antiferromagnetically coupled μ-oxo-bis-[phthalocyanatopyridinemanganese(III)] oligomer[24a] is 1.96 (1) Å.[25]

Table XII summarizes the observed M–N distances for a sequence of metallotetraphenylporphyrins and metallophthalocyanines as a function of atomic number. As noted previously,[5,6] the data for the metalloporphyrins are correlated with the required presence of an electron in the $3d_{x^2-y^2}$ orbital of the d^9 copper(II) atom and the d^5 manganese(II) atom and the absence of such an electron in the $3d_{x^2-y^2}$ orbital of the intermediate-spin iron(II) atom and low-spin cobalt(II) and nickel(II) atoms. The data for the metallophthalocyanines are seen to follow the same pattern except those for MnPc; clearly this derivative must have its $3d_{x^2-y^2}$ orbital empty, corresponding to an intermediate-spin species.

The size of the "central hole" of phthalocyanine complexes is known to be somewhat smaller than those in the analogous porphyrin complexes.[29] Comparison of the Fe and Cu results (Table XII) and data for six-coordinate manganese(III) derivatives[25,30] and tin(IV) derivatives[31,32] leads to a quantitative difference in hole size of 0.046–0.050 Å.[33] Thus the Mn–N bond distance in the *hypothetical* intermediate-spin manganese(II) porphyrin would be ~1.985 Å. Clearly, the existence of an intermediate-spin manganese(II) porphyrin is not precluded on stereochemical grounds. The divergent ground states of MnPc and MnTPP may be the result of differences in the ligand field strengths of the two ligands or possibly the greater flexibility of porphinato ligands in the radial direction. It is worthwhile to point out the distinctiveness of the ligated derivatives of MnPc and MnTPP. MnPc has been reported to add two ligands to form low-spin six-coordinate $MnPcL_2$ species;[24] manganese(II) porphyrins, on the other hand, add only one ligand to form high-spin five-coordinate MnPcL complexes.[6] These results also suggest a greater ligand field strength for the phthalocyanato ligand compared to porphinato ligands.

The pattern of intermolecular contacts in MnPc and FePc is essentially the same as that reported by Brown[13] for CuPc. Of particular interest is the contact between the iron atom and the azamethine nitrogen atom N_1 of an adjacent molecule which is 3.24 Å. The N_1FeN_4 angle is 85.5°; N_1FeN_2 is 89.5°. The corresponding Mn···N_1 contact is 3.18 Å; the N_1MnN_4 angle is 85.2° and the N_1MnN_2 angle is 89.1°. The deviation of N_1 from the mean plane (Figures 1 and 2) is toward the metal atom of the adjacent molecule. It has been suggested[13] that this M···N_1 "interaction" found in the β polymorphs stabilizes this crystal structure.

Acknowledgment. We thank the National Institutes of Health (Grant HL-15627) for partial support of this work and the Computing Center of the University of Notre Dame for computing time.

Registry No. FePc, 132-16-1; MnPc, 14325-24-7.

Supplementary Material Available: Tables X and XI, showing root-mean-square amplitudes of vibration, and listings of structure factor amplitudes (30 pages). Ordering information is given on any current masthead page.

References and Notes

(1) (a) W. Klemm and L. Klemm, *J. Prakt. Chem.*, **143**, 82 (1935); (b) A. B. P. Lever, *J. Chem. Soc.*, 1821 (1965); (c) C. G. Barraclough, R. L. Martin, S. Mitra, and R. C. Sherwood, *J. Chem. Phys.*, **53**, 1643 (1970); (d) H. Miyoshi, H. Ohya-Nishiguchi, and Y. Deguchi, *Bull. Chem. Soc. Jpn.*, **46**, 2724 (1973); (e) H. Miyoshi, *ibid.*, **47**, 561 (1974); (f) A. Hudson and H. J. Whitfield, *Inorg. Chem.*, **6**, 1120 (1967); (g) T. H. Moss and A. B. Robinson, *ibid.*, **7**, 1692 (1968); (h) B. W. Dale, R. J. P. Williams, and T. L. Thorp, *J. Chem. Phys.*, **49**, 3441 (1968); (i) B. W. Dale, R. J. P. Williams, P. R. Edwards, and C. E. Johnson, *ibid.*, **49**, 3445 (1965); (j) B. W. Dale, *Mol. Phys.*, **28**, 503 (1974).

(2) J. M. Robertson, "Organic Crystals and Molecules", Cornell University Press, Ithaca, N.Y. 1953, p 263.

(3) (a) J. M. Robertson and I. Woodward, *J. Chem. Soc.*, 219 (1937); (b) R. P. Linstead and J. M. Robertson, *ibid.*, 1736 (1936); (c) J. M. Robertson, *ibid.*, 615 (1935).

(4) Abbreviations used: Pc, dianion of phthalocyanine; TPP, dianion of *meso*-tetraphenylporphyrin.

(5) J. P. Collman, J. L. Hoard, N. Kim, G. Lang, and C. A. Reed, *J. Am. Chem. Soc.*, **97**, 2676 (1975).

(6) B. Gonzales, J. Kouba, S. Yee, C. A. Reed, J. F. Kirner, and W. R. Scheidt, *J. Am. Chem. Soc.*, **97**, 3247 (1975).

(7) E. G. Meloni, R. L. Ocone, and B. P. Block, *Inorg. Chem.*, **6**, 424 (1967).

(8) H. A. Rutler, Jr., and J. D. McQueen, *J. Inorg. Nucl. Chem.*, **12**, 361 (1960).

(9) N. F. M. Henry and K. Lonsdale, Ed., "International Tables for X-Ray Crystallography", Vol. I, 3d ed, Kynoch Press, Birmingham, England, 1969, p 99.

(10) R. Blessing, P. Coppens, and P. Becker, *J. Appl. Crystallogr.*, **7**, 488 (1974). The validity of estimating backgrounds by this procedure has been checked by collecting two data sets (on another compound), one employing the customary stationary-crystal, stationary-counter backgrounds and the other using profile analysis backgrounds (P. Madura and W. R. Scheidt, to be submitted for publication).

(11) A. C. T. North, D. C. Phillips, and F. S. Matthews, *Acta Crystallogr., Sect. A*, **24**, 351 (1968).

(12) W. R. Scheidt, *J. Am. Chem. Soc.*, **96**, 84 (1974).

(13) C. J. Brown, *J. Chem. Soc. A*, 2488 (1968).

(14) A local modification of ORFLS was employed: W. R. Busing, K. O. Martin, and H. A. Levy, "OR-FLS, a Fortran Crystallographic Least-Squares Program", Report ORNL-TM-305, Oak Ridge National Laboratory, Oak Ridge, Tenn., 1962.

(15) D. T. Cromer and J. B. Mann, *Acta Crystallogr., Sect. A*, **24**, 321 (1968), with real and imaginary corrections for anomalous dispersion in the form factor for iron or manganese from D. T. Cromer and D. Liberman, *J. Chem. Phys.*, **53**, 1891 (1970).

(16) Scattering factors for hydrogen were from R. F. Stewart, E. R. Davidson, and W. T. Simpson, *J. Chem. Phys.*, **42**, 3175 (1965).

(17) The Fourier program ALFF was used: C. R. Hubbard, C. O. Quicksall, and R. A. Jacobson, "The Fast Fourier Algorithm and the Programs ALFF, ALFFDP, ALFFPROJ, ALFFT, and FRIEDEL", Report IS-2625, Ames Laboratory, Iowa State University, Ames, Iowa, 1971.

(18) Supplementary material.

(19) C. K. Johnson, "ORTEP, a Fortran Thermal-Ellipsoid Plot Program for Crystal Structure Illustrations", Report ORNL-3794, Oak Ridge National Laboratory, Oak Ridge, Tenn. 1965.

(20) J. R. Mooney, C. K. Choy, K. Knox, and M. E. Kenney, *J. Am. Chem. Soc.*, **97**, 3033 (1975).

(21) See Table VII in V. W. Day, T. J. Marks, and W. A. Wachter, *J. Am. Chem. Soc.*, **97**, 4519 (1975).

(22) R. G. Little, J. A. Ibers, and J. E. Baldwin, *J. Am. Chem. Soc.*, **97**, 7049 (1975).

(23) T. Kobayashi, F. Kurokawa, T. Ashida, N. Uyeda, and E. Suito, *Chem. Commun.*, 1631 (1971).
(24) (a) G. Englesma, A. Yamamoto, E. Markham, and M. Calvin, *J. Phys. Chem.*, **66**, 2517 (1962); (b) A. Yamamoto, L. K. Philips, and M. Calvin, *Inorg. Chem.*, **7**, 847 (1968).
(25) L. H. Vogt, Jr., A. Zalkin, and D. H. Templeton, *Inorg. Chem.*, **6**, 1725 (1967).
(26) P. Madura and W. R. Scheidt, to be submitted for publication.
(27) A. A. Sayler and J. L. Hoard, to be submitted for publication.
(28) E. B. Fleischer, C. K. Miller, and L. E. Webb, *J. Am. Chem. Soc.*, **86**, 2342 (1964).
(29) T. A. Hamor, W. S. Caughey, and J. L. Hoard, *J. Am. Chem. Soc.*, **87**, 2305 (1965).
(30) J. F. Kirner and W. R. Scheidt, *Inorg. Chem.*, **14**, 2081 (1975).
(31) D. Rogers and R. S. Osburn, *Chem. Commun.*, 840 (1971).
(32) D. M. Collins, W. R. Scheidt, and J. L. Hoard, *J. Am. Chem. Soc.*, **94**, 6689 (1972); D. L. Cullen and E. F. Meyer, Jr., *Acta Crystallogr., Sect. B*, **29**, 2507 (1973).
(33) Strictly speaking, this difference in hole size is only appropriate for quasi-S_4 ruffled metalloporphyrins and planar metallophthalocyanines; the difference in hole size may be increased by 0.020–0.030 Å for a planar metalloporphyrin derivative.

Contribution No. 3519 from the Department of Chemistry, University of California, Los Angeles, California 90024

Preferential Solvation of the Thallous Ion and its Relationship to the Thallium-205 Nuclear Magnetic Resonance Chemical Shift

JAMES J. DECHTER and JEFFREY I. ZINK*

Received October 24, 1975 AIC50773Q

The solvent dependence of the $^{205}Tl(I)$ NMR chemical shift is found to correlate linearly with the solvent's relative solvating ability toward Tl^+. The relative solvating ability is quantitatively measured using the mole fraction dependence of the chemical shift and analyzed by a solvent-exchange equilibrium constant theory. The analysis provides a method of obtaining chemical shifts in solvents that do not dissolve thallous salts. The correlation of solvating ability with the chemical shift is explained by a model utilizing simple symmetry considerations of MO theory. The relative solvating ability determined by Tl NMR is compared to several current thermodynamic models of Lewis acid–base interactions.

Introduction

Investigations of the solvent dependence of the chemical shift of the monovalent ions lithium, sodium, and thallium have usually included an attempt to characterize the chemical shift either by a physical property of the solvent such as pK_a[1] or by empirical solvent parameters such as Gutmann's donor numbers[2-5] or Kosower's Z parameter.[6] Although the general features of the chemical shifts can often be explained by one of the many simplified forms of the Ramsey equation,[7-11] the details of the solvent dependence of the chemical shift are not well understood. In this paper, the solvent-dependent chemical shift for Tl^+ is shown to be linearly related to the relative solvating ability toward Tl^+ of the various solvents. This relation can be understood in terms of the amount of p character produced in the ground state by Tl^+–solvent interactions.

Previous quantifications of preferential solvation have used the isosolvation number[12,13] as a measure of solvating ability. More recently, Covington et al.[14-17] have proposed an expression for the equilibrium constant for a solvent-exchange process. It will be shown (vide infra) that these two measures of relative solvating ability are directly related to each other. Both methods have been applied to the study of the mole fraction dependence of the $^{23}Na^+$ chemical shift.[12,13] $^{205}Tl^+$, with greater sensitivity relative to protons than $^{23}Na^+$, with a much greater solvent-dependent chemical shift range, and with an intense uv absorption band, should be a more convenient probe for studying solvation processes.

The solubility of thallous salts in many types of solvents such as ethers, ketones, and esters is not sufficient to allow the determination of the chemical shift in these solvents. An important consequence of the Covington et al. expression is that Tl^+ chemical shifts can be determined for solvents in which thallous salts have very low solubilities (vide infra). The shifts are determined by using successive approximations in fitting the experimental data to an equilibrium constant.

In this paper quantitative values for the relative solvating ability with respect to Tl^+ of a wide variety of solvents are presented. These values are compared with current empirical thermodynamic models which have been proposed as general measures of solvent–solute interaction. The chemical shift of solvated Tl^+ is shown to be linearly related to the relative solvating ability of the solvent. Finally, a model is presented which describes the solvent-dependent chemical shifts using symmetry considerations of MO theory and explains the latter correlation.

Experimental Section

$TlClO_4$ and TlF were commercially obtained and were recrystallized from deionized water and dried under vacuum over P_2O_5. $TlBF_4$ was prepared by neutralizing a solution of fluoroboric acid with Tl_2CO_3, recrystallizing the product twice from deionized water and drying under vacuum over P_2O_5.

Organic solvents were generally prepared by refluxing over BaO or CaH_2 and then distilled under reduced pressure just prior to use. DMF was refluxed over $MgSO_4$ and distilled.

Instrumental Work. Spectra were obtained using an HR 60 modified with an external field/frequency proton lock. The lock signal was cyclohexane contained in a capillary displaced along the z axis from the sample coils. The lock channel frequency of 55.5 MHz was produced by a crystal and was modulated by a VFO. Maximum lock stability was obtained when the lock channel modulation was 1600 Hz. The observation channel frequency of approximately 32.0 MHz was produced by a frequency synthesizer and could be varied by over 100 kHz to cover the full Tl^+ solvent-dependent chemical shift range. It is modulated by a second VFO; for Tl^+ the observation channel modulation frequency is 3000 Hz.

Fifteen-millimeter o.d. NMR tubes were spun by means of a precision spinner. Chemical shifts are reported in ppm from the infinite dilution resonance of Tl^+ in water.[11] Downfield shifts are positive. No bulk susceptibility corrections are made since these are estimated to be within the experimental error of the shifts.

The resonance line widths were found to vary nearly linearly with chemical shift from about 5 Hz in pyrrole to almost 60 Hz in *n*-butylamine. Because of this variation in line width, the lowest concentration of Tl^+ that could be maintained from solvent to solvent and yet still allow detection of the resonance in the solvents that produce large line widths was 0.20 M.

Fitting Procedure. Equilibrium constants were calculated using the expression derived by Covington et al.[14] shown in eq 1. The various

$$K^{1/n} = \left(\frac{\delta}{\delta_P - \delta}\right)\left(\frac{1-\chi_P}{\chi_P}\right) \quad (1)$$

quantities except n which will be discussed later are illustrated in Figure 1 for the mole fraction dependence of the Tl chemical shift in the